Numerical simulations of thermo-electro-magnetic phenomena in YBCO films subjected to strains

Jing Xia and You-He Zhou*

Department of Mechanics and Engineering Sciences, Lanzhou University, 730000, People's Republic of China
* Corresponding author: zhouyh@lzu.edu.cn

Abstract Due to thermal contractions, tensions and electromagnetic forces, YBCO coated conductors in high-temperature superconductors apparatuses are subjected to mechanical strains. The strains cause the degradation of the critical current densities and influence thermo-electro-magnetic features in the conductors. Based on the dynamic process of thermo-electro-magnetic interaction, we report the results of numerical simulation of thermo-electro-magnetic phenomena in an infinite YBCO film subjected to a uniform in-plane strain in an alternating external magnetic field parallel to the sample surface. The numerical simulation shows the distributions of magnetic induction, electric intensity, current density and temperature in the film and their dependences on the uniform strain. The AC loss in the film is also calculated. We find that whether the magnetic field fully penetrates the superconductor is the key factor to influence the feature of AC loss. When the magnetic field cannot fully penetrate the superconductor the loss rises with increasing strain. When the magnetic field can fully penetrate the superconductor the feature is just opposite.

Keywords YBCO film; thermo-electro-magnetic phenomenon; strain

1. Introduction

The second-generation high-temperature superconductors consisting of a YBCO film deposited on a metallic substrate, referred to as YBCO coated conductors, are promising materials for power applications, such as cables, fault-current limiters and transformers. During the past several years impressive development is being made for the conductors. Very high critical current densities of $2.5-3.0\ \mathrm{MA\,cm^{-2}}$ at $77\ \mathrm{K}$ have been reached in long conductor lengths [1]. Due to thermal contractions, tensions and electromagnetic forces, the coated conductors in high-temperature superconductors apparatuses are subjected to mechanical strains. The strains cause the degradation of the critical current densities and influence thermo-electro-magnetic features in the conductors. But it is impossible to avoid the strains. The effects of strains on the critical current densities have been reported by many researches. However, researches investigating the effects of strains on the other thermo-electro-magnetic features are relatively less. Osami Tsukamoto and his partners have done a series of studies on the AC losses in coated conductors subjected to strains [2-6]. But they have not studied the details of thermo-electro-magnetic phenomena in the coated conductors, such as the distributions of magnetic induction, temperature, electric intensity and current density.

In this paper, we propose an approach to investigate the thermo-electro-magnetic features in an infinite YBCO film subjected to a uniform strain in an external AC magnetic field parallel to the surface of film. The approach is based on numerically solving the coupled magnetic and heat diffusion equations associated with the intrinsic nonlinear behaviors of $\rho(B,T,\varepsilon)$, $J_c(T,B,\varepsilon)$, $c(T)$, etc., from which the details of thermo-electro-magnetic phenomena in the film and their dependences on the strain are obtained.

2. Mathematical model and numerical analysis method

We consider an infinite YBCO film in yz plane with thickness $2d$ in x direction subjected to a uniform strain ε in y direction and an external magnetic field $\mathbf{B}_{ex}$ parallel to the sample

surface in z direction (see Fig. 1).

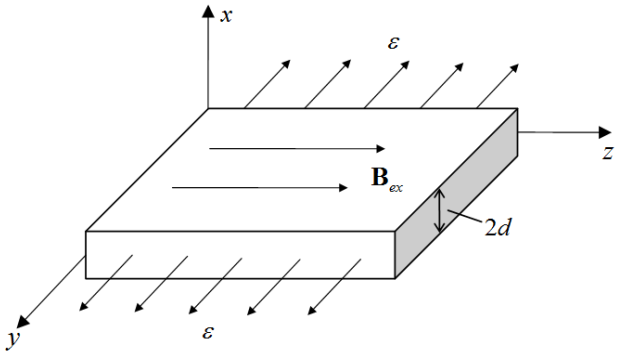

Figure 1. Sketch of the model.

The YBCO film is modeled as a slab, at which the distributions of the z component of magnetic induction $B(x,t)$, the y component of electric intensity $E(x,t)$, and the current density $J(x,t)$ are governed by the Maxwell equations

$$\frac{\partial B}{\partial x}+\mu_0 J=0, \tag{1}$$

$$\frac{\partial B}{\partial t}+\frac{\partial E}{\partial x}=0, \qquad -d\le x\le d. \tag{2}$$

Here， $\mu_0=4\pi\times10^{-7}\ \mathrm{N\,A^{-2}}$ is the permeability of free space. Considering the $E-J$ relation of superconductor can be assimilated with that of normal conductor, i.e.,

$$E=\rho(B,T,\varepsilon)J, \tag{3}$$

where $\rho(B,T,\varepsilon)$ stands for the effective electric resistance, hence Eqs. (1) and (2) can be reduced into the form

$$\frac{\partial}{\partial x}\left(\rho(B,T,\varepsilon)\frac{\partial B}{\partial x}\right)-\mu_0\frac{\partial B}{\partial t}=0, \qquad -d\le x\le d. \tag{4}$$

The temperature $T(x,t)$ is satisfied with one-dimensional Fourier's heat conducting equation

$$\frac{\partial}{\partial x}\left(\kappa\frac{\partial T}{\partial x}\right)-c(T)\frac{\partial T}{\partial t}+W=0, \qquad -d\le x\le d, \tag{5}$$

in which κ represents the thermal conductivity, $c(T)$ is the heat capacity, and $W=EJ$ indicates the heat source intensity. After the YBCO film is cooled to the temperature of the coolant in the zero magnetic field (i.e., the external magnetic field is equal to zero), the boundary and initial conditions of the magnetic field and the temperature field can be written as

$$x=\pm d: \qquad B(x,t)=B_{ex}(t), \tag{6}$$

$$x=\pm d: \qquad \kappa\frac{\partial T}{\partial x}=\pm h(T)(T-T_0), \tag{7}$$

$$t=0: \qquad B(x,t)=0, \qquad T(x,t)=T_0, \tag{8}$$

where $h(T)$ is the heat transfer coefficient，T_0 denotes the temperature of the coolant, and $B_{ex}(t)$ stands for the external magnetic field. Here, we apply a sinusoidal field $B_{ex}(t)=B_0\sin 2\pi ft$.

At the temperature zone of liquid nitrogen，a power law $E=E_c(J/J_c)^{U_0/kT}$ is reasonable for describing electromagnetic constitutive relation of the high-temperature superconductor, where J_c is the critical current density defined by the reference electric field E_c, U_0 denotes the activation energy and k is the Boltzmann constant [7]. According to Eq. (3), the effective electric resistance

ρ is given by

$$\rho(B,T,\varepsilon)=\frac{E_c}{J_c}\left|\frac{J}{J_c}\right|^{U_0/kT-1}. \tag{9}$$

The present research on the activation energy indicates that the energy is dependent on the local temperature and magnetic field, and it is explicitly expressed by [8]

$$U_0(T,B)=U_{00}[1-(T/T_c)^4][1-B/B_{c2}(T)], \tag{10}$$

where U_{00} denotes the barrier height in the zero magnetic field at 0 K, T_c is the critical temperature, and $B_{c2}(T)=B_{c2}(0)[1-(T/T_c)^2]$ stands for the upper critical magnetic field.

For the samples of YBCO, the dependence of the critical current density on strain $J_c(\varepsilon)$ is given by fitting the experimental data with relation [9, 10]

$$J_c(\varepsilon)=J_c(\varepsilon=0)(1-a|\varepsilon|^{2.2}), \tag{11}$$

in which a is the fitting parameter. After the temperature and magnetic field dependence of critical current density is taken into account [11, 12], i.e.,

$$J_c(T,B)=J_{c0}[1+(T/T_c)^2]^{-1/2}[1-(T/T_c)^2]^{5/2}\frac{B^*}{|B|+B^*}, \tag{12}$$

we can get the temperature, magnetic field and strain dependence of critical current density, i.e.,

$$J_c(T,B,\varepsilon)=J_{c0}[1+(T/T_c)^2]^{-1/2}[1-(T/T_c)^2]^{5/2}(1-a|\varepsilon|^{2.2})\frac{B^*}{|B|+B^*}, \tag{13}$$

where the parameter J_{c0} is the critical current density when the temperature, magnetic field and strain are equal to zero, and B^* is a phenomenological parameter.

Consequently, the system with thermo-electro-magnetic interaction can be described by the initial-boundary problem of Eqs. (4)-(8). It is hard to solve the nonlinear coupling problem analytically, so we propose a numerical code by means of the finite difference method and iteration to solve it.

3. Results and discussions

In this section, thermo-electro-magnetic phenomena in the YBCO film subjected to a uniform strain in an external magnetic field parallel to the sample surface at the temperature zone of liquid nitrogen are displayed by the numerical results which are obtained from the essential equations in the previous section. We investigate the distributions of magnetic induction, temperature, electric intensity and current density in the film and their dependences on the uniform strain. Two situations are taken into account. One is that the magnetic field does not fully penetrate the YBCO film. The other one is that the magnetic field fully penetrates the YBCO film. In addition, the AC loss in the film is calculated. In the numerical analysis, we select the parameters in their possible regions given in literatures [9, 13-18]: $a=9900$, $J_{c0}=6.4\times10^{11}$ A m^{-2}, $2d=0.8\times10^{-6}$ m, $T_c=92$ K, $T_0=76$ K, $B_{c2}(0)=200$ T, $U_{00}/kT_0=54$, $B^*=0.3$ T, $E_c=10^{-4}$ V m^{-1}, $h=1$ J m^{-2} s^{-1} K^{-1}, $\kappa=4$ J m^{-1} s^{-1} K^{-1}, $c(T)=2.02\times10^2T^2-7.82\times10^{-3}T^4$ (J K^{-1} m^{-3}). The external magnetic field frequency f is selected as 50 Hz.

3.1. The magnetic field does not fully penetrate the YBCO film

Fig. 2 shows the distributions of the z component of magnetic induction $B(x,t)$, temperature

$T(x,t)$, the y component of electric intensity $E(x,t)$ and current density $J(x,t)$ in the YBCO film at $\varepsilon = 0.2\%$ and $B_0 = 0.001$ T. The curves at different times in a magnetization period T^{cycle} are displayed. When the external magnetic field amplitude B_0 is applied to 0.001 T, the magnetic field cannot fully penetrate the film. From Fig. 2(a), one sees that the magnetic field penetration depth increases with increasing external magnetic field. When $t = T^{cycle}/4$, the external magnetic field gets to the maximum. After the time, the external magnetic field decreases gradually. The magnetic induction in the film near the surface decreases with that. However, the magnetic field penetration depth does not decrease. This is because the pinning force hinders flux lines from moving out of the superconductor. After $T^{cycle}/2$, the external magnetic field increases in the opposite direction. When $t = 3T^{cycle}/4$ the external magnetic field gets to the maximum in the negative direction. The distribution of magnetic induction in the film at this time is just opposite compared with that when $t = T^{cycle}/4$, which means the distributions at the two times have the same values, however, their directions are opposite. The distributions of magnetic induction at $T^{cycle}/2$ and T^{cycle} have the same feature. Fig. 2(b) illustrates the temperature at every position in the film is the same during the magnetization period. Due to the AC loss in the film, the temperature of the film increases with time. But the increments of temperature are slight. From Fig. 2(c), one sees that the distributions of electric intensity are antisymmetrical about the middle layer of the film. At the surface of the film, the values of electric intensity at $T^{cycle}/2$ and T^{cycle} are larger than those at $T^{cycle}/4$ and $3T^{cycle}/4$. This is because the external magnetic field sweep rate $|dB_{ex}/dt|$ at $T^{cycle}/2$ and T^{cycle} is faster than that at $T^{cycle}/4$ and $3T^{cycle}/4$, the vortex electric intensities generated are larger. The current density has the same direction with the electric intensity, so the distributions of electric intensity are also antisymmetrical about the middle layer of the film (see Fig. 2(d)).

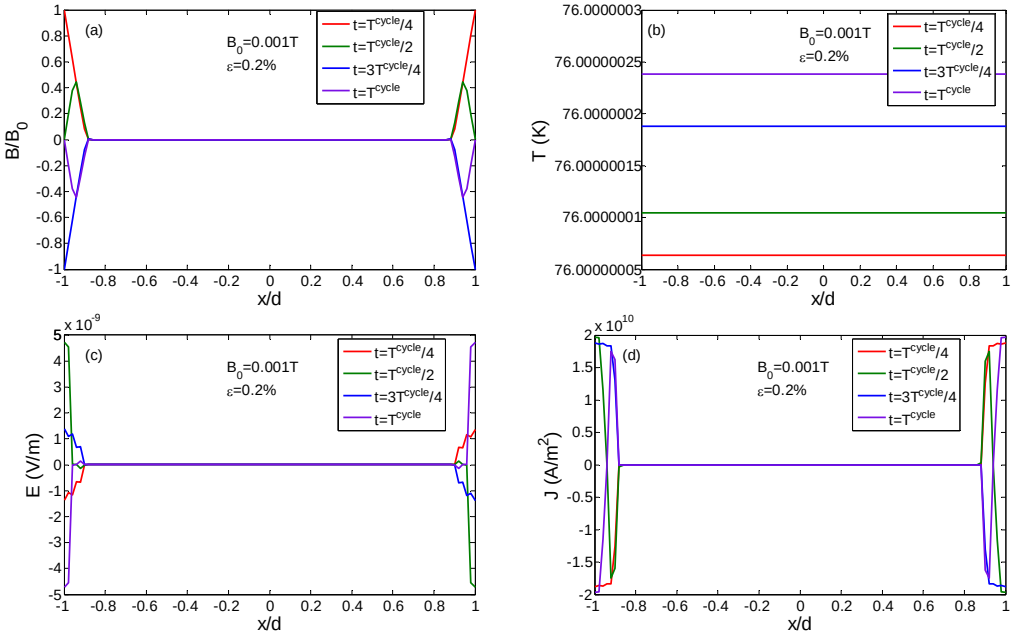

Figure 2. The distributions of the z component of magnetic induction $B(x,t)$, temperature $T(x,t)$, the y component of electric intensity $E(x,t)$ and current density $J(x,t)$ in the YBCO film at $\varepsilon = 0.2\%$ and $B_0 = 0.001$ T. In Fig. 2(a), the magnetic induction B is normalized by the external magnetic field amplitude B_0.

Fig. 3 demonstrates the dependences of the distributions of magnetic induction, temperature, electric intensity and current density on the uniform strain under the situation that the magnetic field does not fully penetrate the film. We find that their dependences on the strain are slight. Fig. 3(a) shows the distributions of magnetic induction at $\varepsilon = 0\%, 0.2\%, 0.4\%$ when the time is equal to $T^{cycle}/4$. One sees that the magnetic induction in the superconducting film increases slightly when the strain increases. According to Eq. (13) the critical current density J_c decreases with increasing strain ε, so the pinning force decreases with increasing strain. When the pinning force decreases, it is easier for the flux lines to move into the superconductor. So the magnetic induction in the film increases. However, the increment is slight, which indicates the effect of strain on the pinning force is very small when the magnetic field does not fully penetrate the film. From Fig. 3(b) and Fig. 3(c), one sees that the strain almost has no effect on the distributions of temperature and electric intensity. The three curves at $\varepsilon = 0\%, 0.2\%, 0.4\%$ superpose. Fig. 3(d) illustrates the current density in the film near the surface decreases with increasing strain. At the deeper position in the film, the feature is opposite. We need to point out that only the range of reversible strain is considered in our simulations. When the strain exceeds the irreversible strain limit ε_{irr} ($\varepsilon_{\text{irr}} = 0.5\%$ in this paper), cracks begin to appear in the superconductor, which result in the irreversible degradation in critical current density [9]. This is not permitted in applications [10, 19, 20].

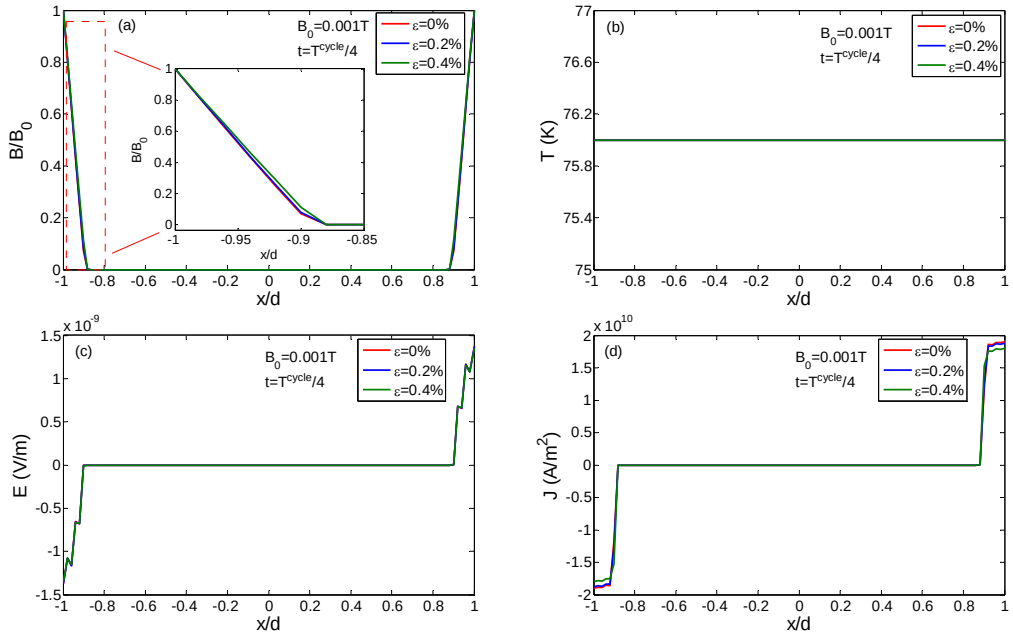

Figure 3. The dependences of the distributions of magnetic induction, temperature, electric intensity and current density on the uniform strain when $B_0 = 0.001$ T. In Fig. 3(b) and Fig. 3(c), the three curves at $\varepsilon = 0\%, 0.2\%, 0.4\%$ superpose.

3.2. The magnetic field fully penetrates the YBCO film

Fig. 4 shows the distributions of magnetic induction, temperature, electric intensity and current density in the YBCO film at different times when $\varepsilon = 0.2\%$ and $B_0 = 0.02$ T. When the external magnetic field amplitude B_0 is applied to 0.02 T, the magnetic field can fully penetrate the film. The features of the evolutions of these distributions with time are similar to those when the magnetic field cannot fully penetrate the film. From Fig. 4(a), one also sees that after $T^{cycle}/4$ although the external magnetic field decreases, the magnetic induction in the film closed to the

middle layer increases. According to this phenomenon, we can deduce the pinning force in the film closed to the middle layer reduces during the decrease of external magnetic field (Fig. 2(a) illustrates the same feature).

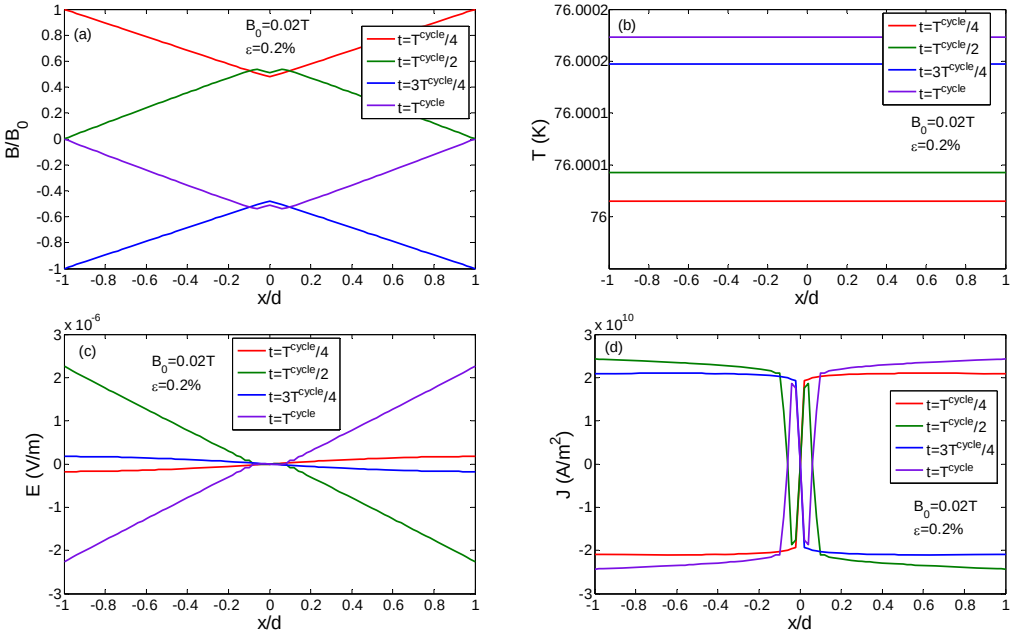

Figure 4. The distributions of magnetic induction, temperature, electric intensity and current density in the YBCO film at $\varepsilon = 0.2\%$ and $B_0 = 0.02$ T.

Fig. 5 demonstrates the dependences of the distributions of magnetic induction, temperature, electric intensity and current density on the uniform strain under the situation that the magnetic field fully penetrates the film. It is found that the effects of strain on these distributions are more obvious than those when the magnetic field does not fully penetrate the film in the range of reversible strain. When the strain increases the AC loss in the film decreases, which results in the decrease of temperature in the film (see Fig. 5(b)). Fig. 5(c) and Fig. 5(d) indicate that the larger the strain is, the smaller the electric intensity and current density are. This feature is different from that when the magnetic field does not fully penetrate the film.

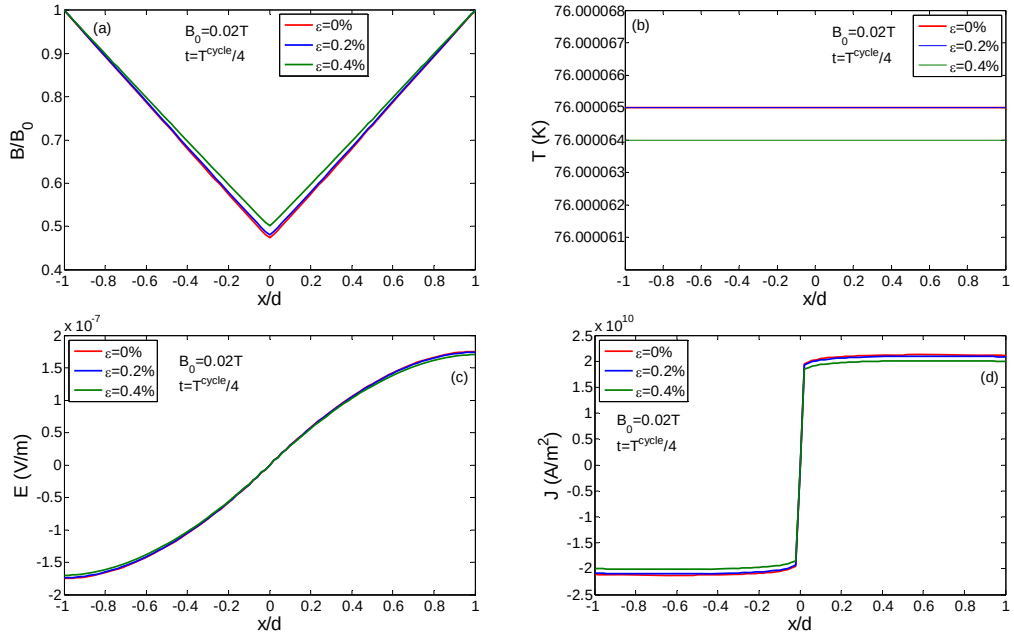

Figure 5. The dependences of the distributions of magnetic induction, temperature, electric intensity and

current density on the uniform strain when $B_0 = 0.02$ T. In Fig. 5(b), the red line and blue line superpose.

3.3. The AC loss in the YBCO film

After $E(x,t)$ and $J(x,t)$ in the YBCO film are numerically obtained, AC loss per unit volume per cycle Q is obtained by the following formula

$$Q = \frac{1}{2d}\int_{T^{\text{cycle}}} \mathrm{d}t \int_{-d}^{d} EJ\mathrm{d}x. \tag{14}$$

Fig. 6 shows curves of the AC loss Q versus the uniform strain ε at different external magnetic field amplitudes. It is interesting to find that when the magnetic field cannot fully penetrate the superconducting film ($B_0 = 0.001$ T), the loss rises with increasing strain. However, the feature is opposite when the magnetic field can fully penetrate the film ($B_0 = 0.02$ T).

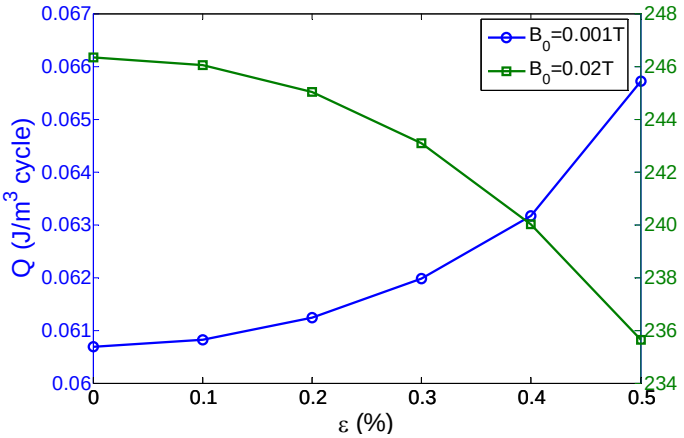

Figure 6. Curves of the AC loss Q versus the uniform strain ε when $B_0 = 0.001$ T and $B_0 = 0.02$ T.

4. Conclusions

By solving the nonlinear coupled equations of magnetic and heat diffusions numerically, we study thermo-electro-magnetic phenomena in an infinite YBCO film subjected to a uniform in-plane strain in an alternating external magnetic field parallel to the sample surface. The distributions of magnetic induction, temperature, electric intensity and current density in the film are investigated at different times under two situations. In one of the situations the magnetic field does not fully penetrate the film and in the other one the magnetic field does. In addition, we investigate the effects of the uniform strain on those distributions. It is found that the effects of the uniform strain are small in the range of reversible strain. At last, the AC loss in the film is reported. We find that whether the magnetic field fully penetrates the superconductor is the key factor to influence the feature of AC loss. When the magnetic field cannot fully penetrate the superconductor the loss rises with increasing strain. When the magnetic field can fully penetrate the superconductor the feature is just opposite.

Acknowledgments

This work was supported by the Fund of Natural Science Foundation of China (Grant No. 11032006; 11121202). We would like to thank Dr Xiaobin Yang for the help on procedure working in this paper.

References

[1] V. Selvamanickam, Y. Chen, X. Xiong, Y. Xie, X. Zhang, Y. Qiao, J. Reeves, A. Rar, R. Schmidt, K. Lenseth, Progress in scale-up of second-generation HTS conductor. Physica C, 463-465 (2007) 482-487.

[2] O. Tsukamoto, A. Kataoka, K. Ohmatsu, AC transport current loss characteristics of REBCO coated conductors subjected to bending strains. IEEE Trans Appl Supercond, 16 (2006) 89-92.

[3] A. Kataoka, O. Tsukamoto, S. Sekizawa, Y. Kawano, N. Kashima, S. Nagaya, Y. Iijima, T. Saitoh, AC transport current loss characteristics of YBCO coated conductors subjected to bending strains. IEEE Trans Appl Supercond, 17 (2007) 3171-3174.

[4] S. Mitsui, T. Uno, S. Maruyama, Y. Nakajima, T. Takao, O. Tsukamoto, AC transport current loss characteristics of copper-stabilized YBCO subjected to repeated mechanical stresses/strains. IEEE Trans Appl Supercond, 20 (2010) 2184-2189.

[5] T. Uno, T. Ojima, S. Mitsui, T. Takao, O. Tsukamoto, AC magnetization losses in copper-stabilized YBCO coated conductors subjected to repeated mechanical stresses. IEEE Trans Appl Supercond, 21 (2011) 3257 - 3260.

[6] O. Tsukamoto, H. Suzuki, Z. Li, M. Ciszek, N. Kashima, S. Nagaya, AC losses in YBCO conductors subjected to tensile stresses. Cryogenics, 47 (2007) 418-424.

[7] E. Zeldov, N.M. Amer, G. Koren, A. Gupta, R.J. Gambino, M.W. McElfresh, Optical and electrical enhancement of flux creep in $YBa_2Cu_3O_{7-\delta}$ epitaxial films. Phys Rev Lett, 62 (1989) 3093-3096.

[8] R. Griessen, Resistive behavior of high-T_c superconductors: Influence of a distribution of activation energies. Phys Rev Lett, 64 (1990) 1674-1677.

[9] D.C. van der Laan, J.W. Ekin, Large intrinsic effect of axial strain on the critical current of high-temperature superconductors for electric power applications. Appl Phys Lett, 90 (2007) 052506.

[10] D.C. van der Laan, J.W. Ekin, J.F. Douglas, C.C. Clickner, T.C. Stauffer, L.F. Goodrich, Effect of strain, magnetic field and field angle on the critical current density of $YBa_2Cu_3O_{7-\delta}$ coated conductors. Supercond Sci Technol, 23 (2010) 072001.

[11] R. Griessen, W. Hai-hu, A.J.J. Van Dalen, B. Dam, J. Rector, H.G. Schnack, S. Libbrecht, E. Osquiguil, Y. Bruynseraede, Evidence for mean free path fluctuation induced pinning in $YBa_2Cu_3O_7$ and $YBa2Cu_4O_8$ films. Phys Rev Lett, 72 (1994) 1910-1913.

[12] M.J. Qin, X.X. Yao, Ac susceptibility of high-temperature superconductors. Phys Rev B, 54 (1996) 7536-7544.

[13] D.C. van der Laan, J.W. Ekin, Dependence of the critical current of $YBa_2Cu_3O_{7-\delta}$ coated conductors on in-plane bending. Supercond Sci Technol, 21 (2008) 115002.

[14] M.K. Wu, J.R. Ashburn, C.J. Torng, P.H. Hor, R.L. Meng, L. Gao, Z.J. Huang, Y.Q. Wang, C.W. Chu, Superconductivity at 93 K in a new mixed-phase Y-Ba-Cu-O compound system at ambient pressure. Phys Rev Lett, 58 (1987) 908-910.

[15] M. Polak, E. Demencik, L. Jansak, P. Mozola, D. Aized, C.L.H. Thieme, G.A. Levin, P.N. Barnes, Ac losses in a YBa2Cu3O7-x coil. Appl Phys Lett, 88 (2006) 232501.

[16] E. Pardo, F. Grilli, Numerical simulations of the angular dependence of magnetization AC losses: coated conductors, Roebel cables and double pancake coils. Supercond Sci Technol, 25 (2012) 014008.

[17] C. Uher, A.B. Kaiser, Thermal transport properties of $YBa_2Cu_3O_7$ superconductors. Phys Rev B, 36 (1987) 5680-5683.

[18] K.-H. Müller, C. Andrikidis, Flux jumps in melt-textured Y-Ba-Cu-O. Phys Rev B, 49 (1994) 1294-1307.

[19] D.C. van der Laan, H.J.N. van Eck, B. ten Haken, H.H.J. ten Kate, J. Schwartz, Strain effects in high temperature superconductors investigated with magneto-optical imaging. IEEE Trans Appl Supercond, 13 (2003) 3534-3539.

[20] M. Sugano, S. Machiya, K. Osamura, H. Adachi, M. Sato, R. Semerad, W. Prusseit, The direct evaluation of the internal strain of biaxially textured YBCO film in a coated conductor using synchrotron radiation. Supercond Sci Technol, 22 (2009) 015002.